Spectrum of resonant plasma oscillations in long Josephson junctions

Thorsten Holst
NKT Research Center, Sognevej 11, DK-2605 Brøndby, Denmark
(Received 2 May 1995)

An analysis is presented for the amplitude of the plasma oscillations in the zero-voltage state of a long and narrow Josephson tunnel junction. The calculation is valid for arbitrary normalized junction length and arbitrary bias current. The spectrum of the plasma resonance is found numerically as solutions to an analytical equation. The low-frequency part of the spectrum contains a single resonance, which is known to exist also in the limit of a short and narrow junction. Above a certain cutoff frequency, a series of high-frequency standing wave plasma resonances is excited, a special feature of long Josephson junctions.

I. INTRODUCTION

The existence of plasma oscillations in the zero-voltage state of Josephson tunnel junctions has been known since the first experimental verification reported by Dahm *et al.*[1] Today, plasma oscillations in short junctions are well understood. The present work deals with the more general case where one of the dimensions of the tunneling area is larger than the characteristic Josephson (magnetic) penetration length λ_J. As a consequence of this extended tunneling structure, the spatial variation of the Josephson phase difference φ is determined by self-field effects which affect the plasma oscillation dynamics.

In any real Josephson junction, different types of resonances exist which originate from the finite size of the tunneling area, i.e., Fiske modes and zero-field modes.[2] Some theoretical considerations concerning plasma oscillations in long Josephson junctions have been published[3] although the resonant properties of the plasma oscillations have not been discussed. Recently, experimental results dealing with the crossover behavior of plasma oscillations in short to intermediate length junctions have been reported.[4]

It is of interest to describe the spectrum of plasma oscillations in long junctions both in its own right and in an attempt to understand more complex dynamics of such nonlinear one-dimensional structures. An example of a related structure is the discrete parallel Josephson junction arrays.[5]

Only small-amplitude plasma oscillations will be analyzed here but the results are valid for arbitrary bias current in the zero-voltage state and for arbitrary junction length.

II. PLASMA OSCILLATIONS

The overlap of two superconducting electrodes separated by an insulating layer defines an electromagnetic transmission line, see Fig. 1. When the Josephson effect is present in such a transmission line, electrons can tunnel between the two electrodes either as electron (Cooper) pairs or as quasiparticles. The long, one-dimensional Josephson junction is given by the condition that the length L of the overlapping electrodes is larger than or comparable to λ_J, while the junction width W is much smaller than λ_J. The governing equation of φ is a perturbed sine-Gordon equation, a nonlinear, partial differential equation which has been used successfully over the last decade to explain experimental data for long Josephson junctions, especially in terms of the dynamics of solitons (fluxons).[6]

In the following, the long Josephson junction is configured in the in-line geometry shown in Fig. 1, where the supplied current only passes through the tunneling barrier at the junction ends. For a junction geometry of the in-line type, the perturbed sine-Gordon equation in its normalized form reads[2]

$$\varphi_{tt}-\varphi_{xx}+\alpha\varphi_t+\sin\,\varphi=0, \tag{1a}$$

with the boundary conditions

$$\varphi_x(\pm l/2,t)=\pm\frac{l}{2}\,(i_0+\varepsilon i_1 e^{i\Omega t}). \tag{1b}$$

Dissipative transport of quasiparticles through the junction is represented by the parameter α. The dc bias i_0 and the oscillating current with amplitude i_1, which is used to probe the plasma resonance in the linear regime, are in units of the critical current I_c. The distance x is normalized to λ_J and the dimensionless junction length is $l=L/\lambda_J$. The frequency $\Omega=\omega/\omega_p^*$ is measured in units of the maximum Josephson plasma frequency $\omega_p^*=\bar{c}/\lambda_J$, where $\bar{c}$ is the speed of light in the junction. Finally, the time coordinate t is normalized to $1/\omega_p^*$.

In the absence of any perturbing probe current, the static profile of the Josephson phase $\varphi_0(x)$ is governed by the equation

$$-\varphi_{0xx}+\sin\,\varphi_0=0, \tag{2a}$$

$$\varphi_{0x}(\pm l/2)=\pm\frac{li_0}{2}. \tag{2b}$$

The perturbative nature of the probe current allows for a linearization of Eq. (1) around the equilibrium background: $\varphi(x,t)=\varphi_0(x)+\varepsilon\varphi_1(x,t)$. Due to the high frequency of the plasma oscillations (typically ranging from 1 to 100 GHz), the main experimental interest is to find the stationary solution of φ_1, which I assume can be written as $\varphi_1(x,t)=a(x)\exp(i\Omega t)$. Insertion of this solution into Eq. (1) gives an equation for the amplitude:

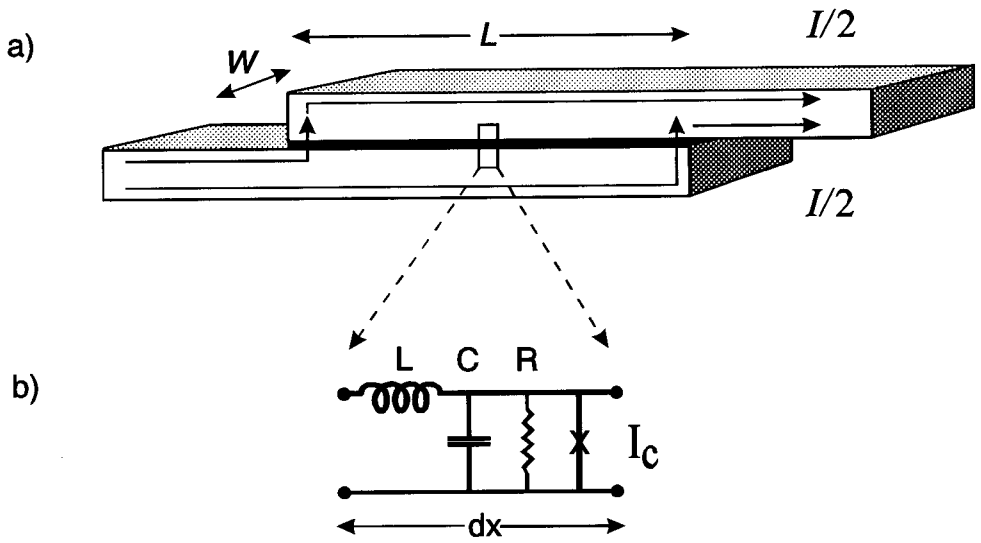

FIG. 1. (a) Schematic drawing of two superconducting electrodes separated by an insulating barrier. The arrows in the electrodes indicate the flow of the bias current I in the in-line geometry. (b) Electrical equivalent diagram where a LC transmission line together with the Josephson effect (ohmic losses R and maximum electron pair current I_c) models the Josephson transmission line.

$$a_{xx}=[\cos\ \varphi_0(x)-\Omega^2+\mathrm{i}\alpha\Omega]a,$$

$$a_x(\pm l/2)=\pm\frac{li_1}{2},$$

which together with Eq. (2) constitute the system of equations to be solved.

The solution of Eq. (2), which has been discussed in details by Owen and Scalapino,[7] is given in terms of Jacobi's elliptic functions sn, cn, and dn:[8]

$$\varphi_{0x}=2\kappa\ \mathrm{cn}(x+x_0|\kappa^2),$$

$$\sin\frac{\varphi_0}{2}=\mathrm{dn}(x+x_0|\kappa^2),$$

where the modulus κ^2 $(0<\kappa^2\leqslant 1)$ and x_0 are integration constants which are to be determined by the boundary conditions given by Eq. (2b). It is simple to verify that $x_0=mK(\kappa^2)$ (K is the complete elliptic integral of the first kind[8] and m is an odd integer) which yields the following relation between the bias current i_0 and the modulus κ_0:

$$i_0=\frac{4\kappa_0(1-\kappa_0^2)^{1/2}\ \mathrm{sn}(l/2|\kappa_0^2)}{l\ \mathrm{dn}(l/2|\kappa_0^2)},$$

together with $\cos\varphi_0(x)=2\kappa_0^2\mathrm{sn}^2(x+mK|\kappa_0^2)-1$. The case $\kappa_0=1$ corresponds to $i_0=0$ and $\varphi_0=0$. Only solutions stationary in time are considered, meaning that the junction is in the (vortex free) zero-voltage state and moving vortex solutions are excluded. The maximum zero-voltage current an inline junction can carry is limited to $i_0^*=\max i_0(\kappa_0)=i_0(\kappa_0^*)$, where the modulus covers the range $\kappa_0^*<\kappa_0\leqslant 1$. As the junction length is increased, the maximum critical current approaches $4/l$, implying that the current carried at both ends of the junction saturates as for example discussed in Ref. 7.

The equation for the amplitude function becomes

$$a_{xx}=[2\kappa_0^2\ \mathrm{sn}^2(x+mK|\kappa_0^2)-1-\Omega^2+\mathrm{i}\alpha\Omega]a,$$

$$a_x(\pm l/2)=\pm\frac{li_1}{2},$$

which is Lamé's equation. The exact analytic solution of this equation may be found in the book of Whittaker and Watson.[9] Following their discussion, the two linearly independent solutions are of the form

$$\frac{H_1(x\mp\tau_0|\kappa_0^2)}{\Theta_1(x|\kappa_0^2)}\exp[\pm Z(\tau_0|\kappa_0^2)x],$$

where H, Θ, and Z are, respectively, the eta, theta, and zeta functions of Jacob,[8] provided the constant τ_0 satisfies the equation

$$1-\mathrm{cn}^2(\tau_0|\kappa_0^2)\mathrm{dn}^2(\tau_0|\kappa_0^2)=(1+\Omega^2-\mathrm{i}\alpha\Omega)\mathrm{sn}^2(\tau_0|\kappa_0^2). \tag{3}$$

Using various identities amongst these functions, Eq. (3) is simplified into

$$\mathrm{cn}(\tau_0|\kappa_0^2)=\frac{(\Omega^2-\mathrm{i}\alpha\Omega)^{1/2}}{\kappa_0}.$$

The parameter τ_0 is given explicitly as $F\{\arccos[(\Omega^2-\mathrm{i}\alpha\Omega)^{1/2}/\kappa_0]|\kappa_0^2\}$, where F is the incomplete elliptic integral of the first kind.

Now the full solution can be written as

$$a(x)=\frac{li_1}{2}\frac{\Theta_1(l/2)}{\Theta_1(x)}\frac{H_1(x-\tau_0)e^{Z(\tau_0)x}+H_1(x+\tau_0)e^{-Z(\tau_0)x}}{\gamma_+e^{Z(\tau_0)l/2}+\gamma_-e^{-Z(\tau_0)l/2}},$$

$$\gamma_\pm=H_1(l/2\mp\tau_0)\Bigg(\pm\kappa_0^2\ \mathrm{sn}(l/2)\mathrm{sn}(\tau_0)\mathrm{sn}(l/2\mp\tau_0)$$

$$-\frac{\mathrm{dn}(l/2\mp\tau_0)\mathrm{sn}(l/2\mp\tau_0)}{\mathrm{cn}(l/2\mp\tau_0)}+\kappa_0^2\frac{\mathrm{sn}(l/2)\mathrm{cn}(l/2)}{\mathrm{dn}(l/2)}\Bigg). \tag{4}$$

If the ohmic loss term is neglected, $\alpha=0$, I can distinguish between two different types of dynamic modes, namely, the following.

Case 1: $\mathrm{cn}(\tau_0|\kappa_0^2)=\Omega/\kappa_0\leqslant 1$. Here τ_0 is real, $0\leqslant\tau_0\leqslant K$, and $Z(\tau_0)$ is real too. Since functions of the form $\exp[\mathrm{i}\Omega t\pm Z(\tau_0)x]$ dominate in the expression for φ_1, the solution has the form of spatially decaying oscillations, where $\lambda=Z^{-1}(\tau_0)$ is a characteristic decaying length for plasma oscillations. I call this the decaying mode. In the absence of bias current, $\kappa_0=1$, I have $\Omega^2=1-\lambda^{-2}$.

Case 2: $\mathrm{cn}(\mathrm{i}\tau_0|\kappa_0^2)=\Omega/\kappa_0\geqslant 1$. Now, $\mathrm{i}\tau_0$ is purely imaginary, $0\leqslant\tau_0\leqslant K'=K(1-\kappa_0^2)$ and consequently $Z(\mathrm{i}\tau_0)$ is purely imaginary. This means that traveling waves of the form $\exp(\mathrm{i}\Omega t\pm \mathrm{i}qx)$ can propagate through the junction, where the wave number $q=\mathrm{Im}Z(\mathrm{i}\tau_0)$ is given by

$$q=\frac{\mathrm{dn}(\tau_0|1-\kappa_0^2)\mathrm{sn}(\tau_0|1-\kappa_0^2)}{\mathrm{cn}(\tau_0|1-\kappa_0^2)}-Z(\tau_0|1-\kappa_0^2)-\frac{\pi\tau_0}{2KK'}.$$

For $i_0=0$, I recover the dispersion relation $\Omega^2=1+q^2$, which is well known from various textbooks on the Josephson effect, e.g., Ref. 2. Note, however, that this dispersion relation is only approached as $O[\mathrm{l/ln}(1-\kappa_0)]$ because of the last term in the expression for q.

The crossover from the decaying to the propagating mode is set by the cutoff frequency

$$\Omega_0=\kappa_0,$$

which also shows the physical meaning of the modulus. Since $0.95<\kappa_0^*<\kappa_0$ for $l>5$, the cutoff frequency is always close to unity in the case of long junctions. In the limit of short junctions, one gets $\kappa_0^*=2^{-1/2}\approx 0.707$.

There are two special cases where the amplitude function and its resonance spectrum can readily be found without the need of the Jacobian functions, namely the cases

$$l=0:\quad a=\frac{i_1}{\Omega_{p0}^2-\Omega^2+\mathrm{i}\alpha\Omega},\quad \Omega_{p0}^4=1-i_0^2,$$

$$i_0=0:\quad a(x)=\frac{li_1\cosh(kx)}{2k\sinh(kl/2)},\quad \Omega_{pn}^2=1+\left(\frac{2n\pi}{l}\right)^2,$$

$$q_n=\frac{2n\pi}{l}, \tag{5}$$

where $k^2=1-\Omega^2+\mathrm{i}\alpha\Omega$. At resonance the standing wave pattern in the junction consists of an integer number n of wavelengths.

III. PLASMA RESONANCE

It is convenient to extract the information contained in the amplitude function in a way, which is more relevant to standard experimental techniques like those used in Refs. 1 and 4. In these works, the junction was biased by a probe signal from a microwave source. A small fraction of the microwave current interacted with the junction and a change in the reflected (or transmitted) microwave signal was observed whenever the plasma oscillation was tuned to resonance. In this way the plasma resonance frequency was mapped out as a function of junction parameters and the input currents.

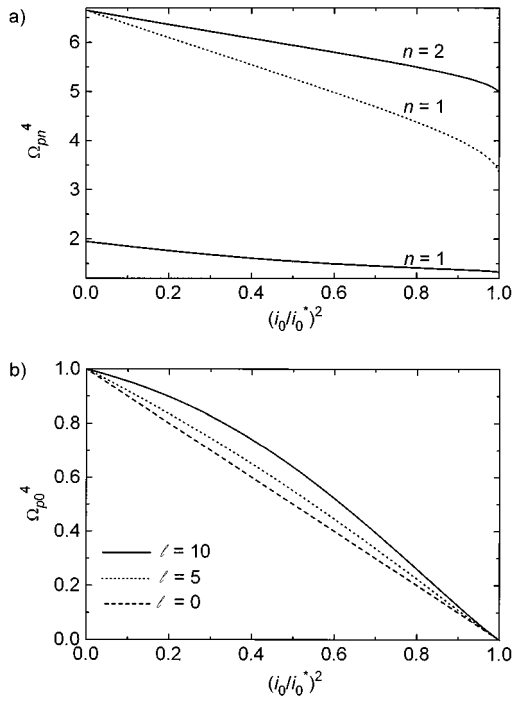

FIG. 2. The plasma resonance is shown as a function of the bias current in the zero-voltage state. (a) Examples of plasma resonances in the propagating mode (standing waves). The integer n indicates the number of wavelengths present in the junction. (b) The plasma resonance in the decaying mode. For an easier comparison, the bias current is shown normalized to the critical current for that specific junction length: $i_0^*(l=0)=1$, $i_0^*(l=5)\approx 0.757$, $i_0^*(l=10)\approx 0.400$.

For the in-line geometry studied here, the probe current is applied to the end of the junction and the reflected (transmitted) signal can be measured at either end of the junction. This only provides information about $a(\pm l/2)$. If appropriate receiver antennas are located along the length of the junction, it may, in principle, be feasible to obtain information about the amplitude of the plasma oscillation at a number of discrete points.

In the case of negligible losses, $\alpha=0$, the plasma resonances are easily recognized as singularities of the amplitude function which are equivalent to solutions of the equation

$$\gamma_+ e^{Z(\tau_0)l/2}+\gamma_- e^{-Z(\tau_0)l/2}=0, \tag{6}$$

with $\gamma_\pm$ given by the expression in Eq. (4). In the following the two different dynamical modes are discussed.

Case 1: Decaying mode. Figure 2(b) shows how the plasma resonance in the decaying mode ($\Omega_{p0}<\Omega_0$) varies as a function of the bias current for various junction lengths. The well-known behavior in the limit of short junctions is a straight line in a plot of Ω_{p0}^4 vs $(i_0/i_0^*)^2$. In the long junction case, due to the decaying nature of this mode the interior part of the junction is only slightly affected by the probe current introduced at the ends. This explains qualitatively why the resonant condition in the case of increasing l tends towards the situation where the static background is spatially more homogeneous and where $\Omega_{p0}=1$. For $l=10$, the shift in plasma resonance frequency accounts for no more than a 5% increase as compared to the short junction case.

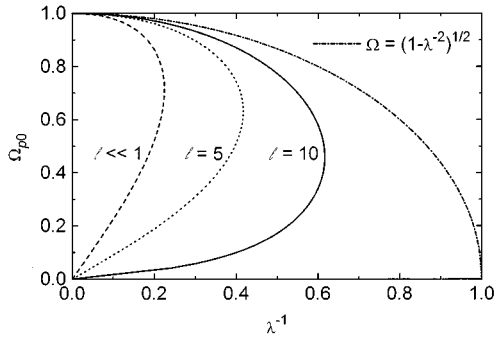

FIG. 3. Plot of the plasma resonance frequency as a function of the inverse decaying length. The dash-dotted line indicates the $\Omega-\lambda^{-1}$ relationship for $i_0=0$.

The $1/e$ decaying length λ calculated at the resonance frequency is plotted in Fig. 3. The spatially most homogeneous amplitude function exists in the vicinity of $i_0\approx 0$ and $i_0\approx i_0^*$. Given the actual λ values, the amplitude function does not exhibit much spatial structure in the decaying mode, since the decaying length is always larger than the Josephson penetration length.

Case 2: Propagating mode. Plasma resonances for the propagating mode, $\Omega_{pn}>\Omega_0$ with $n\geqslant 1$, are special for finite length junctions, contrary to the decaying mode resonance which persists to exist into the short junction limit. Figure 2(a) shows examples of how these standing wave resonances vary with the dc bias. This type of resonance depends weakly on the bias current and is not tuned to zero as i_0 approaches the maximum critical current i_0^*, which is the case for the decaying mode resonance.

In Fig. 4 the dispersion relation is plotted for the case when the junction is tuned to its resonance with the bias current. Also shown is the dispersion relation valid for $i_0=0$, which as mentioned earlier is only approached logarithmically.

IV. DISCUSSION

In the absence of a bias current, the static phase profile is constant in space. When viewing the long Josephson junction as a transmission line this is equivalent to a spatially homogeneous transmission line impedance. At resonance, the nodes of the standing wave pattern are equally spaced along the junction. The spacing between the nodes is a rational fraction of the total junction length as generally known for linear homogeneous transmission lines, see Eq. (5). This is illustrated in Fig. 5 for a normalized junction length of 10.

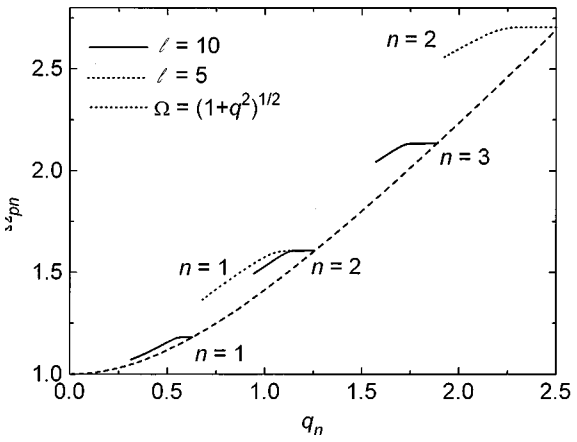

FIG. 4. The dispersion relation plotted at the resonant condition. The dashed line represents the dispersion relation for the case $i_0=0$. The integer n represents the number of wavelengths present in the junction at resonance.

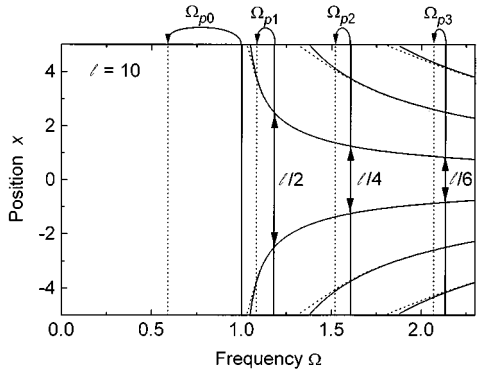

FIG. 5. The curved lines show a contour plot of the nodes where the plasma oscillation amplitude equals zero. The vertical lines indicate the position of the various plasma resonance frequencies. The solid lines are for the case $i_0=0$ and the dotted lines cover the case $i_0=0.95i_0^*$. For both cases, the cutoff frequency is very close to unity, $\Omega_0\approx 1.000$.

When a bias current is applied, the transmission line impedance is no longer independent of the position. Precise knowledge of how the static phase background is set up by the bias current must be incorporated into the analysis in order to trace the resonances, the result being solutions to Eq. (6). From Fig. 5 it is clear that the contour of the nodes changes very little when the bias current is increased towards the critical current. What changes is the spectrum of the resonances. The nodes are no longer exactly equidistant. In the range of interest of the zero-voltage state, $0\leqslant i_0<|i_0^*|$, I find (numerically) that $\Omega_{p0}\leqslant\Omega_0<\Omega_{p1}<\Omega_{p2}<\cdots$, i.e., no change of mode is possible for a given plasma resonance.

In conclusion, the spectrum of the plasma resonance frequency in the zero-voltage state has been calculated for inline Josephson tunnel junctions of arbitrary lengths. From the above analysis, the plasma oscillations naturally fall into two regimes, namely, nearly (spatially) homogeneous oscillations (decaying mode) at low frequencies and standing wave oscillations (propagating mode) above a certain cutoff frequency. Emphasis has been put on presenting the data in a form which is relevant for experimentalists, see Fig. 2. To the best of the author's knowledge, nobody has yet made a direct observation of the plasma resonance in the high-frequency standing wave regime. This should be a straightforward procedure using well-known experimental techniques and would be of interest in testing the predictions of this work.

ACKNOWLEDGMENT

I would like to thank J. Bindslev Hansen for fruitful discussions and for help to improve this text.

[1] A. J. Dahm, A. Denenstein, T. F. Finnegan, D. N. Langenberg, and D. J. Scalapino, Phys. Rev. Lett. **20**, 859 (1968).
[2] K. K. Likharev, *Dynamics of Josephson Junctions and Circuits* (Gordon and Breach, New York, 1986).
[3] P. Lebwohl and M. J. Stephen, Phys. Rev. **163**, 376 (1967); A. L. Fetter and M. J. Stephen, *ibid*. **168**, 475 (1968); A. E. Gorbonosov and I. O. Kulik, Zh. Eksp. Teor. Fiz. **60**, 688 (1971) [Sov. Phys. JETP **33**, 374 (1971)].
[4] T. Holst and J. Bindslev Hansen, Phys. Rev. B **44**, 2238 (1991).
[5] H. S. J. van der Zant, D. Berman, T. P. Orlando, and K. A. Delin, Phys. Rev. B **49**, 12 945 (1994).
[6] E. Jørgensen, V. P. Koshelets, R. Monaco, J. Mygind, M. R. Samuelsen, and M. Salerno, Phys. Rev. Lett. **49**, 1093 (1982); N. Grønbech-Jensen and J. A. Blackburn, *ibid*. **70**, 1251 (1993).
[7] C. S. Owen and D. J. Scalapino, Phys. Rev. **164**, 538 (1967).
[8] M. Abramowitz and I. Stegun, *Handbook of Mathematical Functions*, 9th ed. (Dover, New York, 1970). Note that formula 16.34.3 should read $Z(u)=\pi\vartheta'_3(\pi u/2K)/[2K\vartheta_3(\pi u/2K)]+m\,\mathrm{sn}u\,\mathrm{cn}u/\mathrm{dn}u$.
[9] E. T. Whittaker and G. N. Watson, *A Course of Modern Analysis*, 4th ed. (Cambridge University Press, Cambridge, 1927).